Journal of
Mechanics of
Materials and Structures

ASSESSMENT OF THE MECHANICAL PROPERTIES OF THE NUCLEUS INSIDE A SPHERICAL ENDOTHELIAL CELL BASED ON MICROTENSILE TESTING

Shinji Deguchi, Masayuki Yano, Ken Hashimoto, Hiroyuki Fukamachi, Seiichi Washio and Katsuhiko Tsujioka

Volume 2, Nº 6 June 2007

mathematical sciences publishers

JOURNAL OF MECHANICS OF MATERIALS AND STRUCTURES
Vol. 2, No. 6, 2007

ASSESSMENT OF THE MECHANICAL PROPERTIES OF THE NUCLEUS INSIDE A SPHERICAL ENDOTHELIAL CELL BASED ON MICROTENSILE TESTING

SHINJI DEGUCHI, MASAYUKI YANO, KEN HASHIMOTO,
HIROYUKI FUKAMACHI, SEIICHI WASHIO AND KATSUHIKO TSUJIOKA

The effect of extracellular forces on the nucleus deformation is an important research issue for better understanding of the intracellular force transmission mechanism. Approaches to this issue employing a microtensile test of single cells are helpful because the test enables one to give a well-controlled load onto the specimen with wide force and strain ranges. In the present study, tensile tests of single cells having a spherical shape are conducted by using a microtensile test system with a feedback control of displacement rate. Deformations of the nucleus inside the cell during the cell stretch and subsequent creep recovery after unloading are then quantified based on an image analysis. In order to characterize the creep recovery behaviors of the cell and its nucleus, one-dimensional analytical viscoelastic models and a power-law function are fitted to the creep recovery data. In addition, systematic finite element analyses are performed to estimate the intracellular stress distribution and elastic modulus of the cell and nucleus assumed to be continuum materials. These results indicate that the mechanical behaviors of the nucleus within a cell under stretching and unloading are similar to those under compression loadings previously reported.

1. Introduction

Mechanical forces inherent in the living body are known to regulate physiology and pathogenesis of diseases in addition to chemical factors such as hormones [Davies 1995]. For example, fluid shear stress due to blood flow affects endothelial cells that line the blood vessel and induces antiatherosclerotic functions. In cells, mechanical forces are somehow converted into changes in gene expression leading to such biochemical responses. However, the mechanism by which cells sense forces is still unclear and has been gaining increasing attention from researchers. This is partly because, from a mechanical viewpoint, it remains elusive how externally applied forces are transmitted to intracellular force-sensors including the nucleus that encloses genes [Davies 1995; Janmey 1998; Ingber 2003].

To understand the physical pathway of intracellular force transmission, mechanical behaviors of individual cells [Dong et al. 1991; Karcher et al. 2003; Hashimoto et al. 2004; Desprat et al. 2005; Fernandez et al. 2006; Kasza et al. 2007] and subcellular structural components such as cytoskeletal filaments [Deguchi et al. 2006] and the nucleus [Caille et al. 1998; 2002; Guilak et al. 2000; Dahl et al. 2004; 2005; Tseng et al. 2004; Deguchi et al. 2005a; Rowat et al. 2005; 2006; Vaziri et al. 2006] have been investigated. The cytoskeletal filaments are thin protein fibers used for support of intracellular

Keywords: cell biomechanics, microtensile test, mechanical properties, viscoelastic properties, nucleus, finite element method.
This work was supported in part by the Grants-in-Aid for Young Scientists from the Ministry of Education, Culture, Sports, Science, and Technology in Japan (17700397).

force, cell movement, material transfer within the cell, and so forth. To this end, many experimental approaches that enable to measure the mechanical properties of micron-size biological specimens have ever been developed. In the following two paragraphs, we briefly review such micro and nanomechanical testing techniques: pipette aspiration, atomic force microscopy (AFM) indentation, optical tweezers, and micromechanical test using a pair of microcantilevers.

The pipette aspiration technique uses a small glass tube to aspirate a part of a biological specimen by applying negative pressures inside the tube. The relation between the negative pressures and resultant aspirated lengths of the specimen can give an estimate of the stiffness. This technique was applied to floating cells [Sato et al. 1990] and nuclei isolated from cells [Guilak et al. 2000; Dahl et al. 2004; Deguchi et al. 2005a].

In contrast, the AFM pushes a local part of a biological specimen by using an accurately displaced flexible microcantilever whose stiffness is known in advance. Detection of the cantilever's deflection by the use of an optical technique yields the relation between the indentation lengths and forces loaded onto the specimen surface, giving the stiffness of the specimen. This technique was applied to adherent cells [Haga et al. 2000; Sato et al. 2000] or isolated nuclei [Vaziri et al. 2006]. Employment of analytical [Sato et al. 1990; Haider and Guilak 2000] or computational models [Vaziri et al. 2006] in interpretations of these experimental results can provide more accurate estimations of the mechanical properties. The optical tweezers, introduced by Ashkin et al. [1986], enable a noncontact trapping as well as a manipulation of a specimen by laser radiation pressure. This technique was used to stretch a single cell, by moving trapped beads that attach to the cell, to evaluate mechanical properties [Mills et al. 2004]. A constraint of its low trapping stiffness, however, restricts the maximum generative force to an approximately piconewton order of magnitude.

In the micromechanical test using a pair of microcantilevers, a biological specimen is pulled apart by using a pair of thin needles or microplates [Kishino and Yanagida 1988; Miyazaki et al. 2000; Nagayama et al. 2006; 2007; Deguchi et al. 2006; Desprat et al. 2005], or compressed by microplates [Caille et al. 2002]. By measuring the deflection of the needle or microplate whose stiffness is known in advance, loading-deformation relationship of the specimen can be obtained. Accordingly, the microtensile or compression test is similar to the AFM, but the former is performed in a projected horizontal plane to observe the specimen deformation during the testing. The test can give a large strain, which is different from the pipette aspiration and conventional AFM that can only investigate the effect of a local loading. Hence, this test done in a projected horizontal plane is very useful for evaluation of the mechanical properties at the scale of the whole cell and biological filamentous structure. Also, in contrast to the above-mentioned narrow force range of the optical tweezers, design adjustment of the needle or microplate shape and size enables a force measurement with a wide range from subpiconewton [Kishino and Yanagida 1988] to micronewton [Miyazaki et al. 2000]. Therefore, the technique is more applicable, from the standpoints of strain and force ranges, to a variety of mechanical tests of biological specimen.

We previously developed a microtensile test system using such thin needles with a feedback control [Deguchi et al. 2005b]. The feedback control utilizes a servo system to give an arbitrary magnitude of strain or load as well as a strain rate onto a biological specimen. The system was used for single stress fibers, one of the cytoskeletal filaments, isolated form cells [Deguchi et al. 2006].

In the present study, the system is applied to a single cell, which is larger than the stress fiber in size and probably in force magnitude required for stretching. Deformation behaviors of one of the

principal subcellular structural components, the nucleus, are the subject of much debate. Furthermore, to investigate viscoelastic behaviors of the nucleus and cell, a creep recovery of those materials after unloading was observed.

2. Method

2.1. ***Cell preparation.*** Bovine aortic endothelial cells were cultured in the modified version of Dulbecco's Eagle medium supplemented with 10% fetal bovine serum and 1% each of penicillin and streptomycin. The cells were used at passages 4 and 5 for experiments. Immediately before experiments the cells were rinsed with phosphate buffered saline and treated with trypsin that inhibits cell adhesion. The cells detached from the dish surface were then seeded on a suspension dish containing the culture medium and used for experiments.

2.2. ***Tensile test system.*** Microtensile tests of the individual cells are conducted by using a tensile test system, which we had developed before [Deguchi et al. 2005b] and partially improved for the present study. Briefly, the system was developed on an inverted-microscope (IX-71, Olympus) equipped with two micromanipulators (Narishige) and a CCD camera (Sony) hooked up to an image processor (C3160, Hamamatsu). A floating cell, having a round shape, is captured with a pair of cantilevers displaced by using the micromanipulators as shown in Figure 1. The cantilever, which consists of a carbon fiber and a glass rod, is handmade: a thin carbon fiber having a diameter of 8 μm is attached, with an epoxy adhesive, to the tip of a glass rod having a 1 mm diameter so as to have an appropriate length described below. We prepare two types of the cantilevers by adjusting the carbon fiber length: deflectable and nondeflectable; see Figure 1. For the deflectable cantilever, the length of the carbon fiber located at the tip of a glass rod

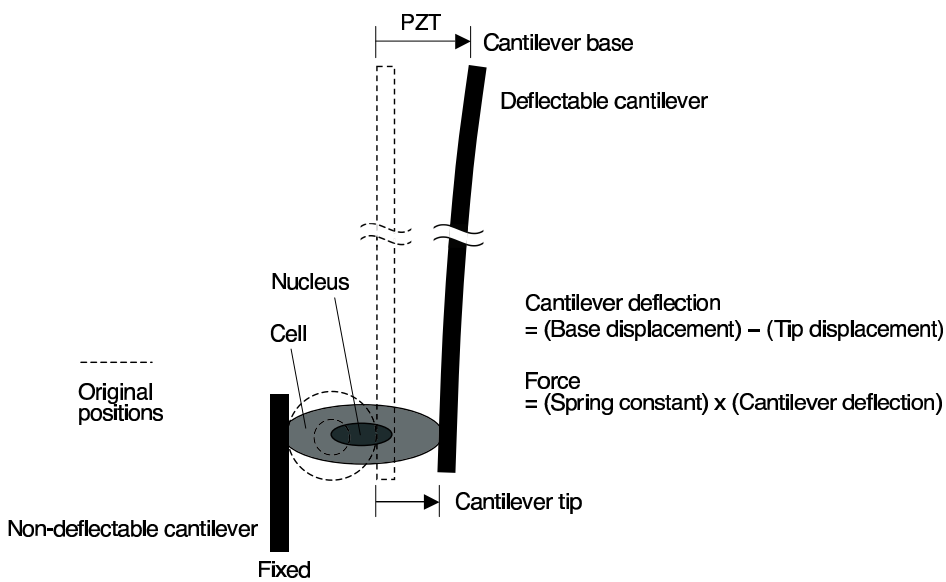

Figure 1. Schematic diagram of the tensile test of a single cell. The cantilever and the cell are not depicted in precise relative scale, and the cantilever deflection is exaggerated.

is set to be ∼2–3 mm. This is so thin that the deflectable cantilever is easily bent. The spring constant for bending of the cantilever is determined by a cross-calibration method [Kishino and Yanagida 1988]. For the nondeflectable cantilever, the carbon fiber is set to have an ∼100 μm length. This is so short that the nondeflectable cantilever has a relatively large value of the spring constant and therefore does not bend against a force that appears in this experiment, approximately less than 10 μN.

In a tensile test a captured cell is stretched by displacing a base part of the deflectable cantilever, while keeping the nondeflectable cantilever unchanged; see Figure 1. The displacement of the deflectable cantilever base is made by a piezoelectric actuator (PZT, NEC Tokin) that is connected to the cantilever base and is driven by a PZT driver controlled by a computer; see Figure 2. A strain-gauge is attached to a surface of the PZT. An extension of the PZT yields a change in the resistance of the strain-gauge, which is detected by a bridge circuit. Thus, we can obtain the displacement of the base part of the deflectable cantilever from the strain-gauge system as shown in Figure 2. Meanwhile, the displacement of the cantilever tip is obtained by the image processor as follows. The cell and the cantilevers are observed during tests by the CCD camera under a halogen light illumination. The image taken by the camera is displayed on a monitor and is also sent to the image processor. The carbon fiber on the tip of the cantilever shuts out a part of the halogen light used to observe the cell. Then, the position of the cantilever tip can be tracked by a binary image processing. The electric outputs, corresponding to the cantilever tip and base displacements, are sent to the computer. Values of the deflection of the cantilever are then obtained by subtracting the tip displacement from the base displacement on a program written in LabVIEW (National Instruments). The tensile force required for stretching the cell is obtained by multiplying the deflection of the cantilever by its spring constant. We can thus obtain the force-displacement relationship of the cell because the displacement of the tip of the deflectable cantilever is equal to that of the stretched cell.

Force-displacement relationship of living tissues is in part affected by strain rate in the mechanical test [Fung 1993]. Although the effect of strain rate on tensile properties is not touched upon in the present study, the experimental setup is expected to have a strain rate control capability in view of a future investigation of the strain rate effect. The tensile test system used in this study adopts a servo control to realize a constant strain rate with a PID controller [Deguchi et al. 2005b]. Prior to the experiment, a desired path for the cantilever tip movement as a function of time is determined and put into the program. Here, a straight line having a constant slope of 1 μm/s is chosen for the desired path. The displacement of the base part of the cantilever, which is the only portion allowed to be directly manipulated by the use of the actuator PZT, is controlled to make the cantilever tip follow the desired path by giving an appropriate input to the PZT driver; see Figure 2. The appropriate input is obtained from the PID controller written in the program, whose optimum gain is determined based on stability according to a calibration conducted

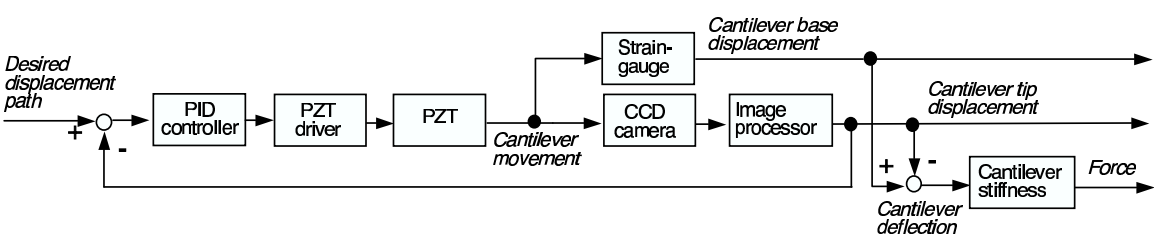

Figure 2. Circuit diagram of the servo system for displacement rate control.

before experiments. Accordingly, the tensile test system enables microtensile tests with an arbitrary strain rate even if the mechanical response of the biological specimen is unknown. This control system is also applicable to a constant loading test for investigating viscoelastic creep behaviors, as reported by other researchers using a similar system [Desprat et al. 2005].

2.3. ***Tensile test.*** Tensile tests of the cells were performed at room temperature (20° C). Before experiments, the tip of the cantilevers was thinly coated with a polyurethane adhesive [Shue and Brozovich 1999; Smith et al. 2000; Nagayama et al. 2006] by using another cantilever having a mass of the adhesive at its tip. The suspension dish containing the floating cells was then mounted on the stage of the microscope. A single cell located at the bottom of the dish was touched at each side by the cantilevers. The targeted cell was held in place for 3 min to strengthen the adhesion between the cell and cantilever. The cell was then lifted up from the bottom carefully. The program is then executed to start a tensile test of the cell. Time course changes in the electric outputs during the tensile test were recorded on the computer and synchronized with video images taken by the camera.

2.4. ***Image analysis.*** The nucleus displacement during the experiment was investigated by image analyses using software (IMAQ, National Instruments). Brightness of each picture element along a survey line was examined. The survey line was selected to cover the whole cell and cantilevers in the direction of the stretch. Positions of the cantilevers and the boundary between the cytoplasm and the nucleoplasm correspond to local minimum brightness points. This allowed us to track the movements of those points.

2.5. ***Finite element analysis.*** A computational cell model was developed in the finite element software (ANSYS) run on a personal computer. Only two separate regions, the cytoplasm and nucleus, were taken into account in the cell model. Here, the cytoplasm and nucleus are both assumed to be continuous, homogeneous, isotropic and hyperelastic materials. Caille et al. [2002] proposed that endothelial cells can be represented as a neoHookean material. They expressed the strain energy function by two parameters, the elastic modulus and Poisson's ratio. We used this model in the finite element analysis of the tensile test. We assumed both the cytoplasm and nucleus are almost incompressible, with Poisson's ratio of 0.48 [Vaziri et al. 2006]. The entire cell and nucleus were both modeled as concentric spheres, with diameters of 21 μm and 10 μm, respectively. To model the fixed cantilever, a part of the left edge of the cytoplasm is fixed in position, while tensile stress is given to a part of the right edge of the cytoplasm. The volume of the fixed or freely moving parts of the cytoplasm is determined from the distance of 17 μm between the cantilevers. Systematic finite element simulations are performed to determine the elastic modulus of the cytoplasm E_c and the nucleus E_n that best fits to experimental data on the cell and nucleus deformations.

3. Results

3.1. ***Tensile properties of the whole cell.*** Single cells were stretched at a constant rate of 1 μm/s by using the feedback control system. A typical example of the test showed that the cell and its nucleus that had round shapes originally were both elongated during the movement of the deflectable cantilever; see Figure 3. We will particularly discuss the nucleus behavior obtained in this example. The cell detached from the right cantilever at 9.5 s after the initiation of the stretch. The detachment occurs at one end of the cell where the adhesion force is probably weaker. The cell shrank soon after the detachment and gradually returned to its original round shape. The electric outputs that represent cantilever displacements indicated

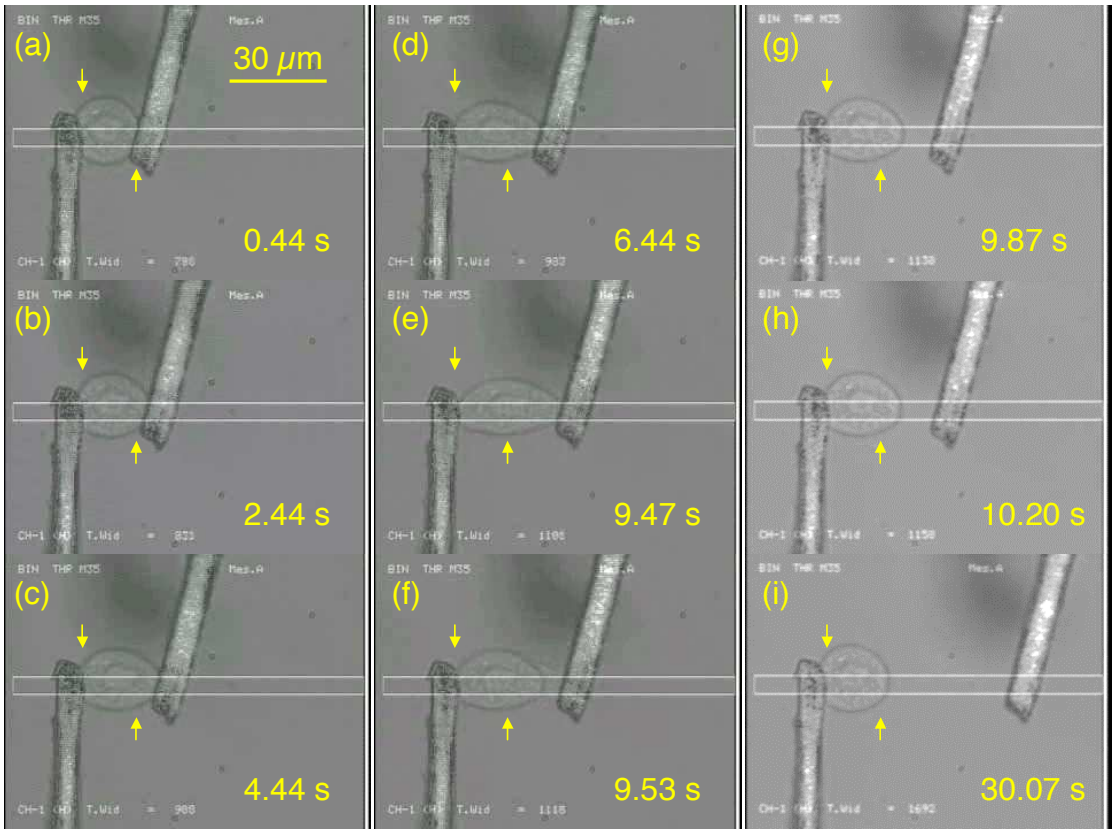

Figure 3. Sequential images of the tensile test and creep recovery after cell unloading. Arrows locate original positions of the inner edges of the cantilevers. White marks originally on the monitor; yellow ones added for clarification. Area within white lines shows where cantilever tip displacement is tracked by binary image processing. Time elapsed given in the lower right of each panel.

that the cantilever tip was displaced at a constant rate of 1 μm/s until the detachment occurred, while the base part showed larger displacements as shown in Figure 4. The constant rise in the cantilever tip displacement, which also corresponds to a constant rise in cell displacement in the longitudinal direction because the left cantilever is fixed, is realized by the feedback control. The difference of the tip and base displacements represents deflection of the right cantilever in bending. The deflection multiplied by the spring constant of 0.14 N/m yields the tensile loading onto the cell; see Figure 5. The tensile loading increased as the stretch proceeded. Here, stretching stain is defined as the ratio of the displacement to the initial longitudinal length of the cell. The initial longitudinal length of the cell is defined to be the original distance between the inner edges of the cantilevers of 17.1 μm. A representative cross-sectional area of the cell is defined as $\pi(D/2)^2$, where $D = 21.1$ μm is the initial lateral diameter of the cell. The original distance between the cantilevers and the initial lateral diameter of the cell were both obtained by an image analysis described in Section 3.2. Stress is defined as the tensile load divided by the above-described

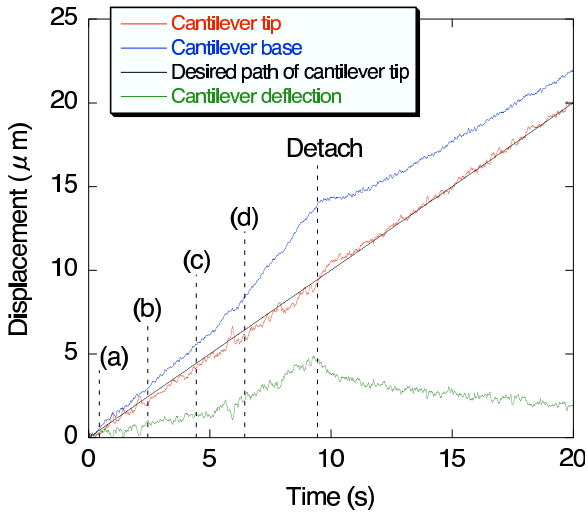

Figure 4. Time course of displacements of deflectable cantilever and its resultant deflection. Moments given by (a)–(d) correspond to those in Figure 3. Regression curve is obtained by the least squares method.

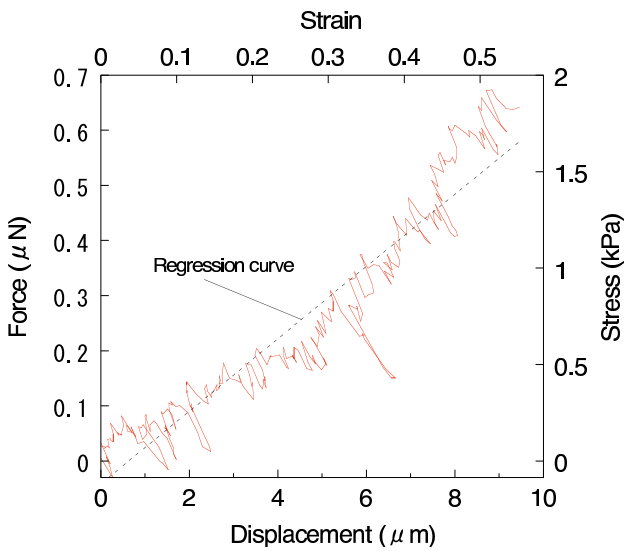

Figure 5. Force-displacement curve of the cell. Right ordinate and upper abscissa show stress and strain, respectively.

representative cross-sectional area calculated using the initial diameter. The ordinate and abscissa of the force-displacement relation are then converted to stress and strain, respectively; see Figure 5. The linear curve obtained by least squares regression to the stress-strain plot provides an estimate of the longitudinal elastic modulus of the cell; for the case of Figure 5 it is 3.2 kPa. The tensile tests were done for 6 cells. The elastic modulus defined above was 2.6 ± 0.7 kPa.

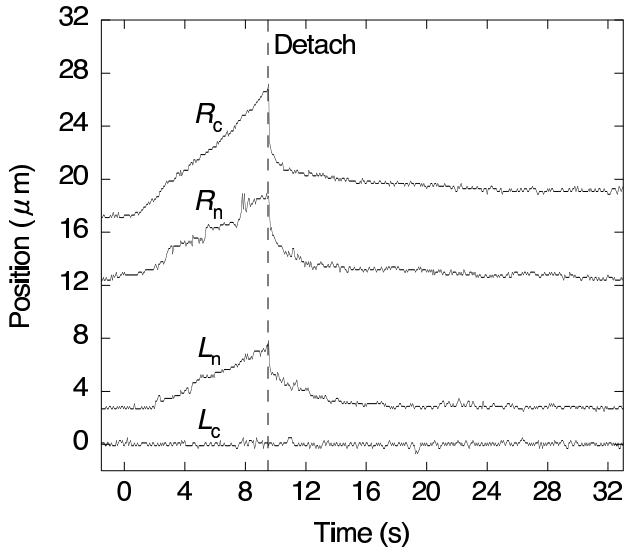

Figure 6. Changes in positions investigated in the image analysis. R_c, L_c are inner edges of the right/left cantilever, respectively, and R_n, L_n are right/left edges of nucleus.

3.2. ***Image analysis of the cell and nucleus behaviors.*** After being detached from the cantilever, the cell gradually deformed owing to viscoelasticity; see Figure 3 for $t > 9.5$. The time course of the deformation during the shrinkage was examined by the image analysis because the electric outputs representing the cantilever positions do not make sense after the detachment; see Figure 4. The image analysis and the subsequent analysis on viscoelasticity were done for the one typical case shown in Figures 3–5. The image analysis result showed that both the cell and the nucleus exhibited shrinkages after detachment and then gradually returned to their original shapes. The right edge of the cell, where the detachment occurred, approached a value different from its original position because the right cantilever originally hid the right part of the cell of length $\sim 1.9\,\mu$m.

3.3. ***Viscoelastic properties.*** From the time course displacements of the cell and nucleus edges obtained in the image analysis shown in Figure 6 the changes in the longitudinal lengths of the cell and nucleus themselves were obtained as shown in Figure 7. After being detached, both the cell and nucleus shrank to their original shapes. In order to study the viscoelastic behaviors we employ the Kelvin or standard linear model, or a power-law function.

The Kelvin model consists of a spring and a dashpot in series, that is, the Maxwell chain, that is placed with a single spring in parallel. The relation between force F and its loading point displacement (u) is represented as [Fung 1993]:

$$F + \tau_\varepsilon \dot{F} = E(u + \tau_\sigma \dot{u}), \tag{1}$$

where E, τ_ε, and τ_σ are constants. It is assumed that the cell is stretched quasistatically at time $t < 0$ and is detached at $t > 0$, which gives

$$u(0^-) = F(0)/E, \qquad t = 0^-, \tag{2}$$

$$F(t) = 0, \qquad t > 0. \tag{3}$$

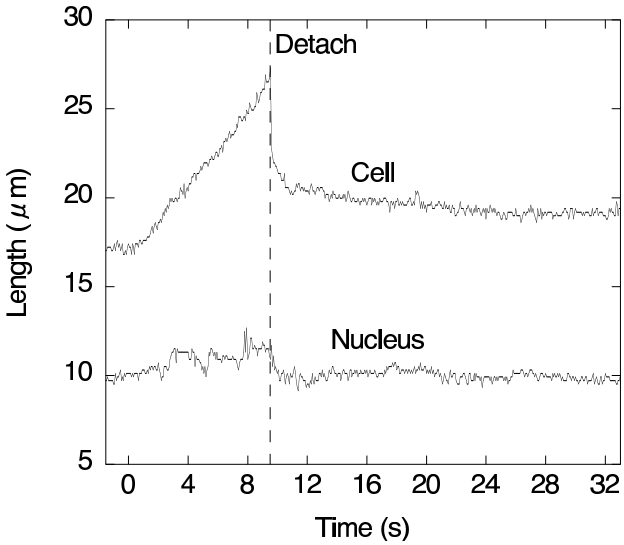

Figure 7. Changes in longitudinal lengths of cell and nucleus during cell stretch.

Integration of Equation (1) considering Equation (3) yields

$$u(t) = u(0^-)\frac{\tau_\varepsilon}{\tau_\sigma}e^{-t/\tau_\sigma}, \quad t \geq 0. \tag{4}$$

Here we assess mechanical properties of the nucleus under an assumption that the time course change in the nuclear deformation shown in Figure 8 is caused by the mechanical properties of the nucleus itself and is independent of the surrounding cytoplasm's influence. Performing a linear fit to the length change before detachment as shown in Figure 7, Equation (2) yields $u(0^-) = 9.6\,\mu$m for the cell and $u(0^-) = 1.6\,\mu$m for the nucleus. These values are then substituted in Equation (4). Assuming τ_ε and τ_σ are separated by a 0.1 s interval, Equation (4) is fitted to the creep recovery data after the unloading of the cell and nucleus to characterize fundamental viscoelasticity of the biomaterials as shown in Figure 8 [Guilak et al. 2000; Vaziri et al. 2006; Nagayama et al. 2007]. A combination of $\tau_\varepsilon = 0.2$ s and $\tau_\sigma = 0.2$ s is best fitted to the nucleus data, suggesting that the nucleus behaved like the Voigt solid instead of the standard linear solid [Fung 1993]. A single combination of τ_ε and τ_σ is not well fitted to the cell data; therefore, two different combinations are analyzed for the earlier and later parts of the data. The right side of Equation (3) plus a value of 1 with a combination of $\tau_\varepsilon = 0.3$ s and $\tau_\sigma = 1.2$ s represents the best fit to the former part of the cell data. A combination of $\tau_\varepsilon = 2.1$ s and $\tau_\sigma = 8.0$ s is the best fit to the latter part of the cell data.

This result suggests that a single use of the Kelvin model might be insufficient for modeling a cell viscoelastic behavior in such a large strain case. The following power-law function is then fitted to the cell creep curve:

$$u(t) = u(0^-)(1 - kt^a), \quad \text{for } t \geq 0, \tag{5}$$

where k and a are constants. A combination of $k = 0.79\,\mu\text{m/s}^{0.071}$ and $a = 0.071$ is the best fit to the curve that was shown in Figure 8, suggesting that a power-law may be an intrinsic feature of cell mechanics [Desprat et al. 2005; Fernandez et al. 2006].

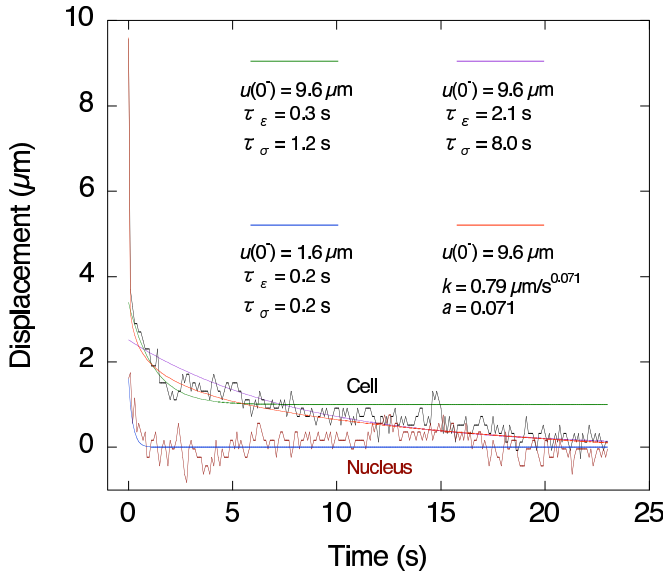

Figure 8. Viscoelastic model fit to displacements of cell and nucleus in creep recovery.

3.4. ***Analytical estimation of tensile properties of the nucleus.*** Force-displacement relation of the nucleus was roughly estimated under an assumption that the force detected by the cantilever was loaded onto the nucleus in the longitudinal stretching direction; see Figure 9. This assumption is similar to the one in a previous study [Maniotis et al. 1997] and is made to obtain a crude estimation, but its effectiveness is tested by finite element method in the following section. Similarly to the case of the cell (Figure 5), strain of the nucleus is defined as the ratio of the displacement to its initial length in the longitudinal direction, which is 9.95 μm. Stress in the nucleus is defined as the force divided by a representative cross-sectional area, given by $A = \pi(D_{\text{lateral}}/2)^2 = \pi(9.95/2)^2$. The right ordinate and the upper abscissa of the force-displacement relation are also represented by the stress and the strain, respectively; see Figure 9. The slope of a linear curve obtained by least squares method for the stress-strain curve provides an estimate of an elastic modulus of 28.2 kPa. For comparison, the regression curve of the force-displacement relation of the cell is shown for the left ordinate and the lower abscissa. In addition, the regression curve of the stress-strain relation of the cell is shown for the right ordinate and the upper abscissa.

3.5. ***Further estimation of the cell and nucleus elastic modulus by finite element analysis.*** Systematic finite element simulations were performed to further estimate the elastic modulus of the cytoplasm E_c and the nucleus E_n. The longitudinal displacements (in the x-direction in Figure 10b) of the cell D_c and the nucleus D_n were computed taking various parameter values of E_c and E_n at 0.2 kPa and 2 kPa intervals, respectively; see Figure 11. D_c was calculated from the changes in the distance between cantilevers in the x-direction. The experimental data just before the detachment shows that tensile loading was 0.58 μN (Figure 5), $D_c = 9.6\,\mu$m and $D_n = 1.6\,\mu$m (Figure 7). The tensile stress, given by tensile loading of 0.58 μN divided by cross-sectional area at the interface between the cell model and the right cantilever 38π μm^2, was given to the right edge of the computational cell model; see Figure 10. The parameter

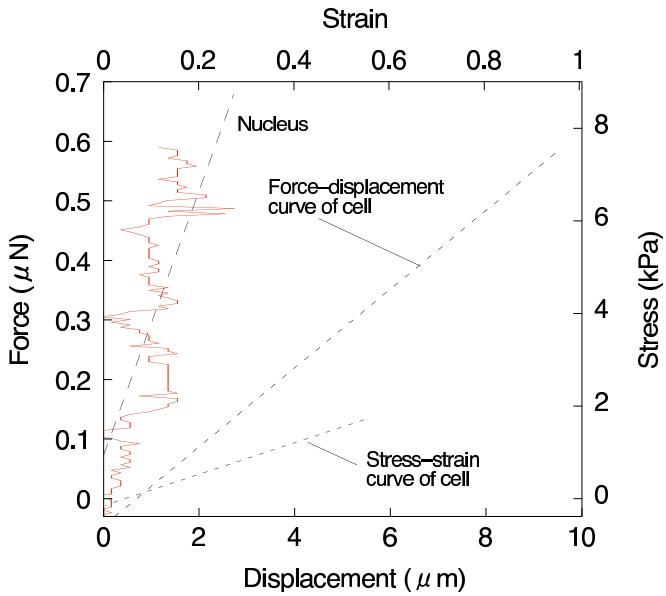

Figure 9. Force-displacement curve of the nucleus. Right ordinate and upper abscissa show stress and strain, respectively. For comparison, regression curve of force-displacement relation of cell is shown for left ordinate and lower abscissa. Regression curve of stress-strain relation of cell is shown for right ordinate and upper abscissa.

combination of E_c and E_n, which results in $D_c = 9.6\,\mu$m and $D_n = 1.6\,\mu$m, was analyzed. The result shows that a combination of $E_c = 3.7$ kPa and $E_n = 32$ kPa represents the best fit; see Figure 11.

4. Discussion

The most significant data obtained in this study is the behavior of the nucleus under unidirectional cell stretching and creep recovery after unloading (Figures 8–11). The tensile properties of the nucleus were first assessed under a rough assumption (Figure 9) that the force detected by the cantilever deflection was loaded onto the nucleus in the longitudinal direction. The estimated elastic modulus was 28.2 kPa, which is 8.8 times stiffer than that of the cell at ~ 3.2 kPa. This value is comparable in magnitude to the result reported by Maniotis et al. [1997], in which nuclei within adherent cells have a rigidity of 9 times stiffer than that of the cytoplasm when a local part of the cell membrane is pulled by using a thin glass needle. Caille et al. [2002] also reported the similar ratio of 10 times. Our result showed a good agreement with the previous studies even in the stretch of the whole portion of a cell.

The elastic modulus is further investigated by finite element analyses of the tensile test (Figures 10 and 11). The effective stress distribution (Figure 10b) shows that there is a distinct stress gradient along the lateral direction vertical to the stretch. This lateral stress gradient is in part caused by a lateral compression of the nucleus by the surrounding cytoplasm. This result indicates that the assumption done in the rough estimation, that is, only force detected by the cantilever deflection is loaded onto the nucleus, may lead to underestimate the elastic modulus of the nucleus. A parametric study employing a spherical cell shape model yielded a larger value of 32 kPa compared with 28.2 kPa that was obtained in

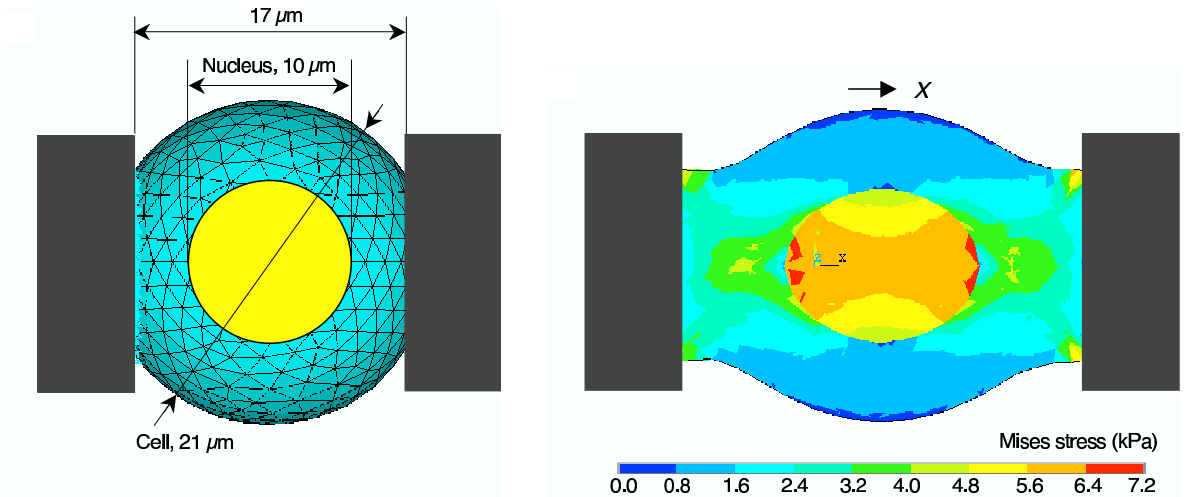

(a) (b)

Figure 10. Finite element simulation of tensile test. (a) Model geometry: the cantilevers as a rigid wall. Cell meshes represent those viewed from outside, and nucleus geometry inside cell is superimposed on top. (b) Effective (von Mises) stress field in center section at a cytoplasm and nucleus elastic moduli $E_c = 3.6$ kPa, $E_n = 34$ kPa, respectively.

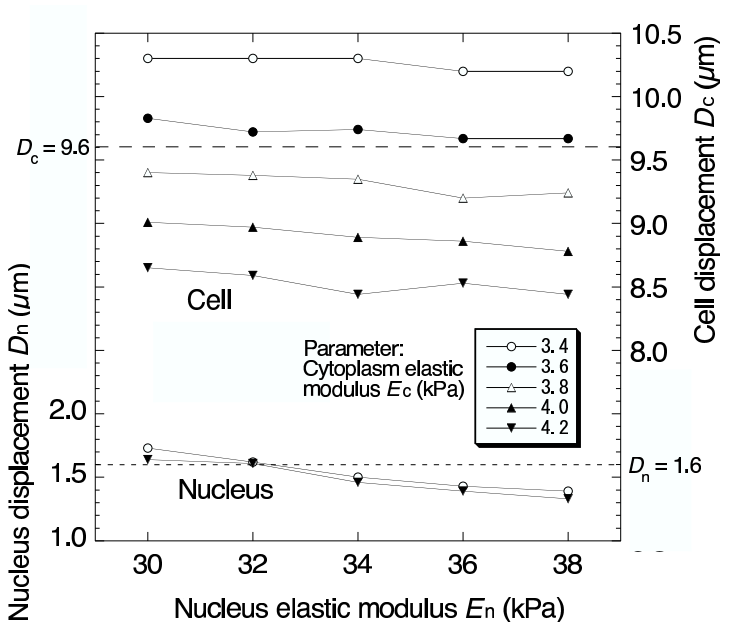

Figure 11. Computational results of the effect of two parameters, cytoplasm and nucleus elastic moduli E_c and E_n, on longitudinal displacements of cell D_c and nucleus D_n.

the simple analysis. A larger elastic modulus estimation of the cytoplasm 3.7 kPa was also obtained in the finite element analysis compared with 3.2 kPa obtained in the analytical estimation. This is caused by that stress was determined, in the rough estimation, from the initial cross-sectional area that is actually reduced gradually as stretch proceeds. Thus, computational continuum mechanics approaches can give an accurate assessment, from a macroscopic view, of the mechanical properties of cell and nucleus, rather than a simple analytical approach. Cells actually have an inhomogeneous structure composed of cytoskeletal networks and membrane-bound organelles. More accurate intracellular force transmission taking the inhomogeneous cell structure into account will be the subject of future investigation [Deguchi et al. 2005c].

The viscoelastic properties of the nucleus in the creep recovery process were assessed under the assumption that the time course change in the nuclear deformation is caused by the mechanical properties of the nucleus and is independent of an influence due to the surrounding cytoplasm. The numerical approach to the viscoelastic behaviors taking the spherical geometry into account will be an issue in the future investigation. Our result indicated that the nucleus behaved like the Voigt solid, whereas the whole cell behaved as a power-law viscoelastic material; see Figure 8. Specifically, the cell exhibited a rapid and large drop in the stretching strain immediately after the detachment and then gradually returned to its original shape. Such a gradual decrease after the detachment was not observed in the nucleus. This is consistent with the observation by Caille et al. [2002] that isolated endothelial nuclei returned elastically to their original morphology when compressing load was removed.

In contrast, Guilak et al. [2000] reported that the nuclei isolated from chondrocytes were nearly as viscous as the cytoplasm using the pipette aspiration technique. In addition, recently increasing knowledge of the mechanical properties of individual nucleus components [Dahl et al. 2004; 2005; Rowat et al. 2005; 2006] suggests nonlinear behaviors of the nucleus. Although the difference between the results is unclear, it may be due to differences in the specimen and experimental condition, for example, the loaded range applied to investigate the viscoelasticity.

The microtensile test requires a quite difficult technique (for example, to capture a small cell by using a pair of cantilevers carefully like chopsticks) compared with a well-developed system of AFM or other mechanical testing approaches [Wang et al. 1993; Karcher et al. 2003; Tseng et al. 2004] that are readily available. This may restrict the use of the microtensile test. Despite the issue, the microtensile test can elucidate nucleus responses within the cytoplasm in a well-controlled tensed state and in an unloaded state, while measuring the force required for stretching. The order of magnitude of the force in the present study was 0.1–1 μN, which is larger than optical tweezers can realize, that is, $\sim$ 10 pN [Mills et al. 2004].

Previous microtensile tests using thin cantilevers revealed that single actin filaments and the actin-bundled stress fibers require a tensile force of piconewton order [Kishino and Yanagida 1988] and nanonewton order [Deguchi et al. 2006], respectively, to be stretched. It is thus possible for the microtensile test to do such a wide force range measurement by adjusting the spring constant of the force-detection cantilever including a microplate used in [Caille et al. 2002]. In addition, the microtensile test enables evaluation of the mechanical properties at a whole cell level with a large strain range, whereas the AFM or other methods can give a limited strain to a local part of a targeted cell.

5. Conclusion

Deformation behaviors of the nucleus during creep recovery after unloading show that the nucleus behaved like the Voigt solid, whereas the whole cell showed a power-law behavior. In addition, under a crude assumption that the tensile force loaded onto the cell is concentrated entirely onto the nucleus, tensile properties of the nucleus are compared with those of the cell. Also, systematic finite element analysis was conducted to make another estimation of elastic modulus of the cell and nucleus. These results indicate that the nucleus is stiffer and more elastic compared with the whole cell subjected to unidirectional stretching and unloading, thereby demonstrating inhomogeneous stiffness and viscoelasticity within a single cell.

Acknowledgements

The authors would like to thank Yoshihiko Tamura (Okayama University) for his help in constructing the experimental setup.

References

[Ashkin et al. 1986] A. Ashkin, J. M. Dziedzic, J. E. Bjorkholm, and S. Chu, "Observation of a single-beam gradient force optical trap for dielectric particles", *Opt. Lett.* **11**:5 (1986), 288–290.

[Caille et al. 1998] N. Caille, Y. Tardy, and J. J. Meister, "Assessment of strain field in endothelial cells subjected to uniaxial deformation of their substrate", *Ann. Biomed. Eng.* **26**:3 (1998), 409–416.

[Caille et al. 2002] N. Caille, O. Thoumine, Y. Tardy, and J. J. Meister, "Contribution of the nucleus to the mechanical properties of endothelial cells", *J. Biomech.* **35**:2 (2002), 177–187.

[Dahl et al. 2004] K. N. Dahl, S. M. Kahn, K. L. Wilson, and D. E. Discher, "The nuclear envelope lamina network has elasticity and a compressibility limit suggestive of a molecular shock absorber", *J. Cell Sci.* **117** (2004), 4779–4786.

[Dahl et al. 2005] K. N. Dahl, A. J. Engler, J. D. Pajerowski, and D. E. Discher, "Power-law rheology of isolated nuclei with deformation mapping of nuclear substructures", *Biophys. J.* **89** (2005), 2855–2864.

[Davies 1995] P. F. Davies, "Flow-mediated endothelial mechanotransduction", *Physiol. Rev.* **75**:3 (1995), 519–560.

[Deguchi et al. 2005a] S. Deguchi, K. Maeda, T. Ohashi, and M. Sato, "Flow-induced hardening of endothelial nucleus as an intracellular stress-bearing organelle", *J. Biomech.* **38**:9 (2005), 1751–1759.

[Deguchi et al. 2005b] S. Deguchi, K. Ohashi, and M. Sato, "Newly designed tensile test system for in vitro measurement of mechanical properties of cytoskeletal filaments", *JSME Int. J. C Mech. Syst. Mach. Elem. Manuf.* **48** (2005), 396–402.

[Deguchi et al. 2005c] S. Deguchi, T. Ohashi, and M. Sato, "Intracellular stress transmission through actin stress fiber network in adherent vascular cells", *Mol. Cell. Biomech.* **2**:4 (2005), 205–216.

[Deguchi et al. 2006] S. Deguchi, T. Ohashi, and M. Sato, "Tensile properties of single stress fibers isolated from cultured vascular smooth muscle cells", *J. Biomech.* **39**:14 (2006), 2603–2610.

[Desprat et al. 2005] N. Desprat, A. Richert, J. Simeon, and A. Asnacios, "Creep function of a single living cell", *Biophys. J.* **88** (2005), 2224–2233.

[Dong et al. 1991] C. Dong, R. Skalak, and K. L. P. Sung, "Cytoplasmic rheology of passive neutrophils", *Biorheology* **28** (1991), 557–567.

[Fernandez et al. 2006] P. Fernandez, P. A. Pullarkat, and A. Ott, "A master relation defines the nonlinear viscoelasticity of single fibroblasts", *Biophys. J.* **90** (2006), 3796–3805.

[Fung 1993] Y. C. Fung, *Biomechanics: mechanical properties of living tissues*, Springer, New York, 1993.

[Guilak et al. 2000] F. Guilak, J. R. Tedrow, and R. Burgkart, "Viscoelastic properties of the cell nucleus", *Biochem. Biophys. Res. Commun.* **269**:3 (2000), 781–786.

[Haga et al. 2000] H. Haga, S. Sasaki, K. Kawabata, E. Ito, T. Ushiki, and T. Sambongi, "Elasticity mapping of living fibroblasts by AFM and immunofluorescence observation of cytoskeleton", *Ultramicroscopy* **82**:1-4 (2000), 253–258.

[Haider and Guilak 2000] M. A. Haider and F. Guilak, "An axisymmetric boundary integral model for incompressible linear viscoelasticity: application to the micropipette aspiration contact problem", *J. Biomech. Eng. (Trans. ASME)* **122**:3 (2000), 236–244.

[Hashimoto et al. 2004] K. Hashimoto, N. Kataoka, E. Nakamura, H. Asahara, Y. Ogasawara, K. Tsujioka, and F. Kajiya, "Direct observation and quantitative analysis of spatiotemporal dynamics of individual living monocytes during transendothelial migration", *Atherosclerosis* **177**:1 (2004), 19–27.

[Ingber 2003] D. E. Ingber, "Tensegrity, I: Cell structure and hierarchical systems biology", *J. Cell Sci.* **116**:7 (2003), 1157–1173.

[Janmey 1998] P. A. Janmey, "The cytoskeleton and cell signaling: component localization and mechanical coupling", *Physiol. Rev.* **78**:3 (1998), 763–781.

[Karcher et al. 2003] H. Karcher, J. Lammerding, H. Huang, R. T. Lee, R. D. Kamm, and M. R. Kaazempur-Mofrad, "A three-dimensional viscoelastic model for cell deformation with experimental verification", *Biophys. J.* **85** (2003), 3336–3349.

[Kasza et al. 2007] K. E. Kasza, A. C. Rowat, J. Liu, T. E. Angelini, C. P. Brangwynne, G. H. Koenderink, and D. A. Weitz, "The cell as a material", *Curr. Opin. Cell Biol.* **19**:1 (2007), 101–107.

[Kishino and Yanagida 1988] A. Kishino and T. Yanagida, "Force measurements by micromanipulation of a single actin filament by glass needles", *Nature* **334**:6177 (1988), 74–76.

[Maniotis et al. 1997] A. J. Maniotis, C. S. Chen, and D. E. Ingber, "Demonstration of mechanical connections between integrins, cytoskeletal filaments, and nucleoplasm that stabilize nuclear structure", *P. Natl. Acad. Sci. USA* **94** (1997), 849–854.

[Mills et al. 2004] J. P. Mills, L. Qie, M. Dao, C. T. Lim, and S. Suresh, "Nonlinear elastic and viscoelastic deformation of the human red blood cell with optical tweezers", *Mol. Cell. Biomech.* **1**:3 (2004), 169–180.

[Miyazaki et al. 2000] H. Miyazaki, Y. Hasegawa, and K. Hayashi, "A newly designed tensile tester for cells and its application to fibroblasts", *J. Biomech.* **33**:1 (2000), 97–104.

[Nagayama et al. 2006] K. Nagayama, Y. Nagano, M. Sato, and T. Matsumoto, "Effect of actin filament distribution on tensile properties of smooth muscle cells obtained from rat thoracic aortas", *J. Biomech.* **39**:2 (2006), 293–301.

[Nagayama et al. 2007] K. Nagayama, S. Yanagihara, and T. Matsumoto, "A novel micro tensile tester with feed-back control for viscoelastic analysis of single isolated smooth muscle cell", *Med. Eng. Phys.* **29**:5 (2007), 620–628.

[Rowat et al. 2005] A. C. Rowat, L. J. Foster, M. M. Nielsen, M. Weiss, and J. H. Ipsen, "Characterization of the elastic properties of the nuclear envelope", *J. Roy. Soc. Interface* **2**:2 (2005), 63–69.

[Rowat et al. 2006] A. C. Rowat, J. Lammerding, and J. H. Ipsen, "Mechanical properties of the cell nucleus and the effect of emerin deficiency", *Biophys. J.* **91** (2006), 4649–4664.

[Sato et al. 1990] M. Sato, D. P. Theret, L. T. Wheeler, N. Ohshima, and R. M. Nerem, "Application of the micropipette technique to the measurement of cultured porcine aortic endothelial cell viscoelastic properties", *J. Biomech. Eng. (Trans. ASME)* **112** (1990), 263–268.

[Sato et al. 2000] M. Sato, K. Nagayama, N. Kataoka, M. Sasaki, and K. Hane, "Local mechanical properties measured by atomic force microscopy for cultured bovine endothelial cells exposed to shear stress", *J. Biomech.* **33**:1 (2000), 127–135.

[Shue and Brozovich 1999] G. H. Shue and F. V. Brozovich, "The frequency response of smooth muscle stiffness during Ca^{2+}-activated contraction", *Biophys. J.* **76**:5 (1999), 2361–2369.

[Smith et al. 2000] P. G. Smith, C. Roy, S. Fisher, Q. Huang, and F. V. Brozovich, "Cellular responses to mechanical stress: selected contribution: mechanical strain increases force production and calcium sensitivity in cultured airway smooth muscle cells", *J. Appl. Physiol.* **89**:5 (2000), 2092–2098.

[Tseng et al. 2004] Y. Tseng, J. S. Lee, T. P. Kole, I. Jiang, and D. Wirtz, "Micro-organization and viscoelasticity of the interphase nucleus revealed by particle nanotracking", *J. Cell Sci.* **117**:10 (2004), 2159–2167.

[Vaziri et al. 2006] A. Vaziri, H. Lee, and M. R. Kaazempur Mofrad, "Deformation of the cell nucleus under indentation: mechanics and mechanisms", *J. Mater. Res.* **21** (2006), 2126–2135.

[Wang et al. 1993] N. Wang, J. P. Butler, and D. E. Ingber, "Mechanotransduction across the cell surface and through the cytoskeleton", *Science* **260** (1993), 1124–1127.

Received 15 Sep 2006. Accepted 27 Feb 2007.

SHINJI DEGUCHI: deguchi@mech.okayama-u.ac.jp
Graduate School of Natural Science and Technology, Okayama University, Tsushima-naka 3-1-1, Okayama 700-8530, Japan

MASAYUKI YANO: *Graduate School of Natural Science and Technology, Okayama University, Tsushima-naka 3-1-1, Okayama 700-8530, Japan*

KEN HASHIMOTO: khashimo@med.kawasaki-m.ac.jp
Department of Physiology, Kawasaki Medical School, 577 Matsushima, Kurashiki, Okayama 701-0192, Japan

HIROYUKI FUKAMACHI: hiroyuki@keilab.mech.okayama-u.ac.jp
Graduate School of Natural Science and Technology, Okayama University, Tsushima-naka 3-1-1, Okayama 700-8530, Japan

SEIICHI WASHIO: washio_s@mech.okayama-u.ac.jp
Graduate School of Natural Science and Technology, Okayama University, Tsushima-naka 3-1-1, Okayama 700-8530, Japan

KATSUHIKO TSUJIOKA: tsujioka@med.kawasaki-m.ac.jp
Department of Physiology, Kawasaki Medical School, 577 Matsushima, Kurashiki, Okayama 701-0192, Japan